

****Volume Title****

*ASP Conference Series, Vol. **Volume Number***

****Author****

© ****Copyright Year**** *Astronomical Society of the Pacific*

The CO-H₂ Conversion Factor in Galaxy Mergers

Desika Narayanan^{1, 2}

¹*Steward Observatory, University of Arizona*

²*Bart J Bok Fellow*

Abstract. The CO-H₂ conversion factor in galaxies is typically described as bimodal: one value for discs and quiescent regions, and another (lower) value for mergers and starbursts. In this proceeding, I will describe both empirical observational evidence that the conversion factor varies with physical environment, as well as a theoretical model which aims to understand the physical processes which drive these variations. I present a functional form for X_{CO} which can be applied to observations ranging in scale from ~ 70 pc to galaxy-wide scales, and show the consequences of the application of this model to the Kennicutt-Schmidt star formation law.

1. Introduction

Deriving an H₂ gas mass from a giant molecular cloud (GMC) or galaxy full of clouds involves the usage of tracer molecules such as ¹²CO (hereafter, CO). This is because H₂ has no permanent dipole moment, and its first quadrupole moment lies ~ 500 K above ground, significantly warmer than the typical ISM temperature in a GMC. Converting from a CO emission line strength to an underlying H₂ gas mass involves the usage of a CO-H₂ conversion factor.

The CO-H₂ conversion factor goes by two names in the literature: X_{CO} ¹ and α_{CO} . The former has units of $\text{cm}^{-2}/\text{K}\text{-km s}^{-1}$, while the latter $\text{M}_{\odot} \text{pc}^{-2}(\text{K}\text{-km s}^{-1})^{-1}$. The two are equivalent, and simply related via $X_{\text{CO}} = 6.3 \times 10^{19} \alpha_{\text{CO}}$ in the aforementioned units. Since both X_{CO} and α_{CO} are used in the literature, I will present the results of this proceeding in terms of both units.

Observationally determining an X-factor requires deriving an independent measurement of H₂ gas mass, and comparing this to an observed CO line flux. Via a variety of methods (some of these are summarised in the seminal conference proceeding by Solomon & Barrett 1991), it has been found that the conversion factor is roughly constant in the Galaxy and nearby galaxies (when the metallicity is of order solar) with value $X_{\text{CO}} = 2 - 4 \times 10^{20} \text{cm}^{-2}/\text{K}\text{-km s}^{-1}$, or $\alpha_{\text{CO}} \approx 3 - 6 \text{M}_{\odot} \text{pc}^{-2} (\text{K}\text{-km s}^{-1})^{-1}$ (for a reference list of these observations, please see the introduction of Narayanan et al. 2011b).

However, despite the seeming constancy of the X-factor in relatively “normal” GMCs, observations of nearby ultraluminous infrared galaxies (ULIRGs) show that the usage of a Milky Way X_{CO} in these environments would cause the inferred H₂ gas mass to exceed the measured dynamical mass (Downes & Solomon 1998). Hence, in

¹ X_{CO} is also referred to as the X-factor. I will use X_{CO} or the X-factor arbitrarily in this proceeding.

ULIRGs, the X -factor must be lower than within the Galaxy. In Figure 1, we show the distribution of X_{CO} and α_{CO} values from the Downes & Solomon (1998) survey, as well as a shaded region for the typical range of Galactic values. There is a dispersion amongst the ULIRG X -factors, though on average they are lower than the Galactic mean. Despite the observed dispersion in ULIRG conversion factors, the fact that they are lower on average than the Milky Way value has led the community to largely adopt a bimodal picture of X_{CO} : a value of $\alpha_{\text{CO}} \approx 4$ for disc galaxies, and $\alpha_{\text{CO}} \approx 0.8$ for starbursts and mergers.

The ramifications of a bimodal form of the CO-H₂ conversion factor are significant. As an example, Daddi et al. (2010a) and Genzel et al. (2010) demonstrated the effects of assuming a bimodal X_{CO} on the Kennicutt-Schmidt (KS) star formation rate-gas density relation. While in $\Sigma_{\text{SFR}} - \Sigma_{\text{CO}}$ space, galaxies at low and high- z lie on an arguably unimodal relation, the introduction of a bimodal X_{CO} to convert the CO luminosity to an H₂ gas mass causes the KS relation to become bimodal. That is, mergers and discs lie on different tracks on the KS relation when utilising a different X_{CO} for each. This is shown explicitly in Figure 2, where I have compiled the galaxies presented in Daddi et al. (2010a) and Genzel et al. (2010), and plotted (in the left panel) the $\Sigma_{\text{SFR}} - \Sigma_{\text{CO}}$ relation, and (in the middle panel), the $\Sigma_{\text{SFR}} - \Sigma_{\text{H}_2}$ relation which utilises a bimodal X -factor. The mergers (squares) and discs (circles) occupy different tracks. This has given rise to a terminology in the literature, as well as at conferences (including this one!), that mergers and discs have different “modes” of star formation. Mergers, according to this relation, form stars more efficiently (i.e. needing less gas to sustain a given SFR) than discs. We will neglect the right panel of Figure 2 for now, and will return to it shortly.

2. The Case Against a Bimodal Conversion Factor: Empirical Observational Evidence

The usage of a bimodal CO-H₂ conversion factor raises a number of difficult questions. For example, if one ascribes a mean “merger/starburst” value of X_{CO} to all mergers, should this value vary with the interaction stage of a merger? What about with close pairs which do not have overlapping discs? Does the same “merger/starburst” value apply for mergers of all gas fractions, orientation angles, star formation rates, mass ratios and galaxy masses? Does this merger value evolve with redshift, or should one utilise the locally-calibrated X -factor for mergers at high- z (which are presumably more gas rich and have higher star formation rates than their local counterparts)? Which value should one use for $z \sim 2$ discs, which are forming stars at rates comparable to local mergers?

An alternative picture to the bimodal X -factor is one in which the CO-H₂ conversion factor varies with the physical conditions in the ISM. Intuitively, this scenario makes sense. The fraction of hydrogen in molecular form, fraction of carbon in the form of CO, and escape of CO radiation from GMCs is all dependent on the physical conditions of the ISM. So, why shouldn’t the CO-H₂ conversion factor also depend on the physical conditions? In fact, there is substantial empirical evidence that it does.

First, as is shown in the Appendix of Tacconi et al. (2008), X_{CO} is seen to vary smoothly with the H₂ surface density of galaxies. This was found by Ostriker & Shetty

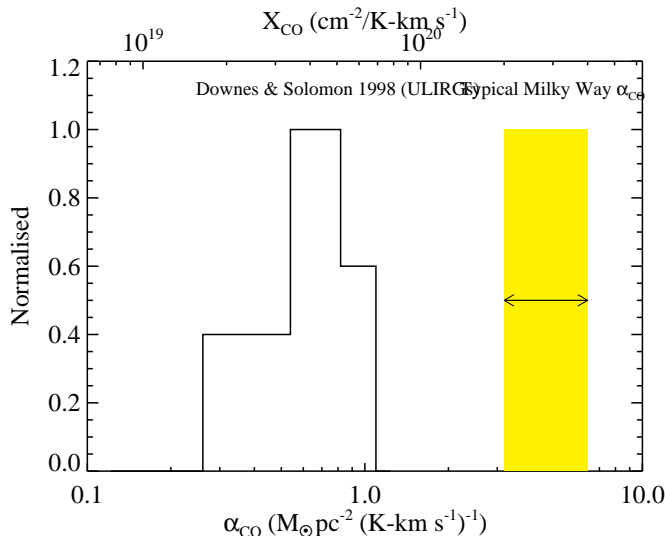


Figure 1. Histogram of the CO-H₂ conversion factors measured for local ULIRGs by Downes & Solomon (1998) (solid black line). The yellow shaded region denotes the typical values found in the Milky Way. Despite a dispersion of conversion factor values for mergers, a singular value of $\alpha_{\text{CO}}=0.8$ is typically assumed for merging galaxies.

(2011) to be well fit by a relation $\alpha_{\text{CO}} \sim \Sigma_{\text{H}_2}^{-0.52} \sim W_{\text{CO}}^{-0.34}$ where Σ_{H_2} is the surface density of molecular gas, and W_{CO} is the observed CO intensity (in K-km s⁻¹).

Second, the X-factor appears to vary with the metallicity of the gas. Recent work by Bolatto et al. (2008), Leroy et al. (2011) and Genzel et al. (2011) has shown that X_{CO} increases with metallicity with power $X \propto (\text{O}/\text{H})^{-b}$ where $b = 1 - 2.7$ (Arimoto et al. 1996; Israel 1997). The physical motivation behind this sort of scaling is that in low metallicity clouds, H₂ can self-shield for survival from photodissociating radiation whereas CO requires some amount of dust to protect it. Hence, the fraction of CO-dark H₂ mass rises as metallicity decreases (Wolfire et al. 2010).

Right away, the results from Ostriker & Shetty (2011) alongside the aforementioned results regarding the variation of X_{CO} with metallicity imply an empirical relation which looks like:

$$X_{\text{CO}} \propto \alpha_{\text{CO}} \propto W_{\text{CO}}^{-\beta} Z^{-b} \tag{1}$$

3. A Theory for the CO-H₂ Conversion Factor

3.1. Numerical Models

We will utilise numerical simulations to try to understand the origins of variations in the CO-H₂ conversion factor. The principle equations for this model are described in Narayanan et al. (2011a), and I encourage the reader to refer to this paper. The description here will be necessarily abbreviated owing to space limitations. We first model the evolution of idealised galaxies hydrodynamically utilising the publicly available SPH code GADGET-3 (Springel 2005). We model isolated disc galaxies, and galaxy mergers over a range of masses, merger mass ratios, and redshifts. We smooth the physical conditions onto an adaptive mesh for the purposes of radiative transfer.

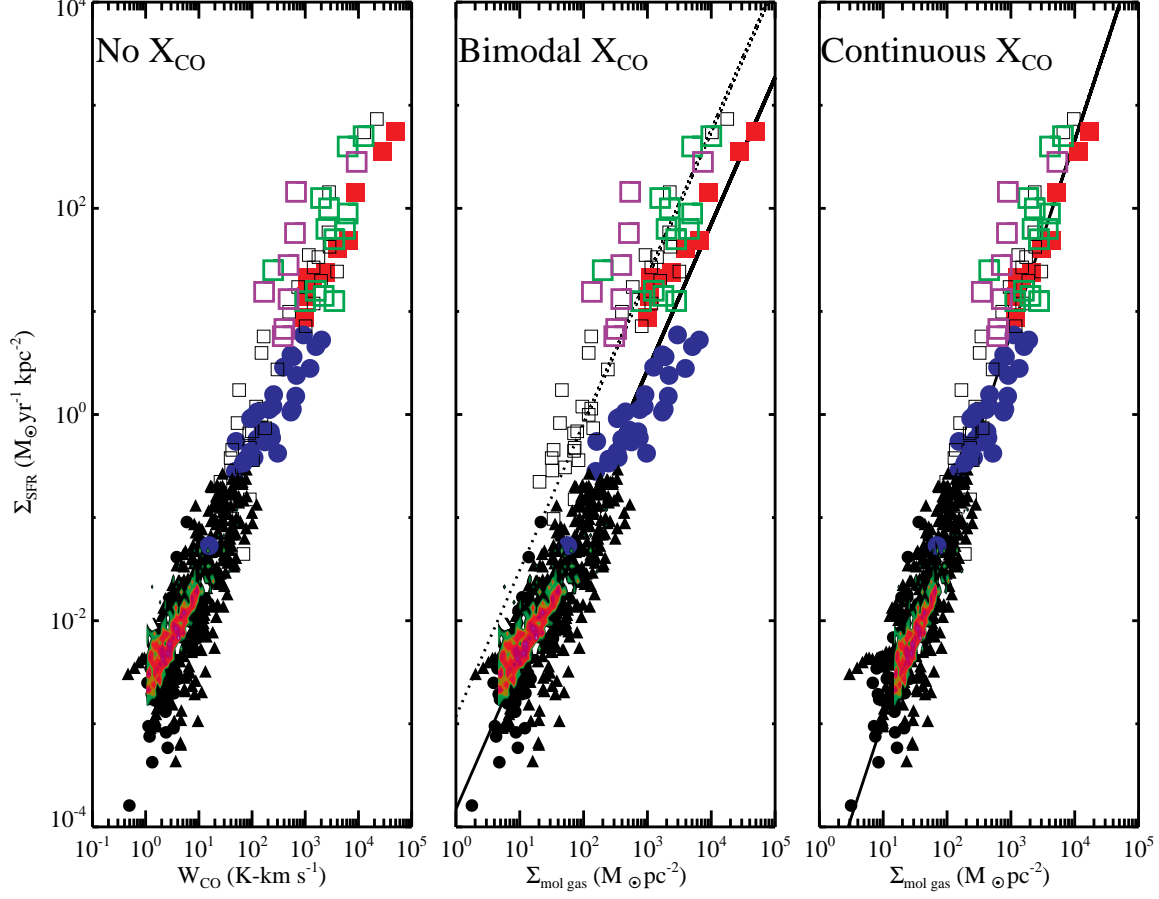


Figure 2. Kennicutt-Schmidt star formation relation in observed galaxies. Circles and triangles are local discs or high- z BzK galaxies (inferred high- z discs), and squares are inferred mergers (local ULIRGs or high- z SMGs). Colours denote surveys galaxies are pulled from and are described in Narayanan et al. (2011b). *Left*: SFR surface density vs. velocity-integrated CO intensity. In terms of the observable, W_{CO} , a unimodal SFR relation exists. *Centre*: When applying an effectively bimodal X_{CO} ($\alpha_{\text{CO}} = 4.5$ for local discs, 3.6 for high- z discs, and 0.8 for mergers), the resulting SFR relation is bimodal, with mergers occupying a track of higher star formation efficiency (defined as $\text{SFR}/M_{\text{H}_2}$). The solid and dotted lines overplotted are the best fit tracks for each “mode” of star formation as published in Daddi et al. (2010a). *Right*: Resulting SFR relation when applying Equation 2 to the data. When X_{CO} varies smoothly with galactic physical properties, the result is a unimodal SFR relation. In this case the power-law index in the relation is approximately 2 (when assuming that each galaxy has metallicity $Z' = 1$).

The H_2 fraction is calculated following the prescriptions of Krumholz et al. (2008, 2009) which balances the photodissociation by Lyman-Werner band photons against growth on dust grains. We assume that all H_2 gas is assumed to be in spherical GMC. Because some cells (which contain little H_2 mass) can be rather large in the adaptive mesh, we establish a floor surface density of $100 M_\odot \text{pc}^{-2}$. In our model mergers, the bulk of the molecular mass is in GMCs which are above this floor value. We move beyond the 10,000 K floor temperature established in GADGET-3 by calculating the temperature of the molecular gas as a balance between line cooling, heating by the grain photoelectric effect, cosmic rays, and energy exchange with dust (Krumholz et al. 2011).

To calculate the CO emission line fluxes, we first determine the emergent radiation from each GMC utilising the publicly available escape probability code of Krumholz & Thompson (2007). We then run the 3D Monte Carlo radiative transfer package *TURTLEBEACH* (Narayanan et al. 2008) to calculate the radiative transfer through the galaxy. With modeled CO line fluxes, and knowledge of the H_2 content in our model galaxies, we are prepared to study the CO- H_2 conversion factor in our simulations.

3.2. Results from Simulations

At a given metallicity, X_{CO} decreases with increasing gas temperature and velocity dispersion. The reason for this is straightforward. The velocity integrated CO line intensity enters X_{CO} in the denominator. As gas temperature increases, the peak intensity of the CO emission line, which is in the Rayleigh-Jeans limit, also increases. Similarly, because GMCs are typically optically thick, as the gas velocity increases, the velocity integrated CO line intensity increases.

This is the reason X_{CO} is lower in galaxy mergers than the Galactic mean value (Narayanan et al. 2011a). In a galaxy merger, the velocity dispersion of the model GMCs in our simulations increase from the virial velocity of the GMCs due to the turbulent nature of the gas in a galaxy merger. The velocity dispersion within a GMC in the merger can be as large as $50 - 100 \text{ km s}^{-1}$ (compared to a few km s^{-1} in a quiescent cloud). Similarly, the gas temperature goes up in GMCs. While the typical temperature of a quiescent GMC is of order $\sim 10 \text{ K}$, representative of the floor temperature established by a Galactic cosmic ray heating rate, the temperatures in GMCs in galaxy mergers can be of order $\sim 50 - 100 \text{ K}$. The reason for this is due to energy exchange with dust. When gas densities rise above $\sim 10^4 \text{ cm}^{-3}$, dust and gas exchange energy extremely efficiently, and the gas temperature rises to the dust temperature (Goldsmith 2001). In a merger, not only are these large gas densities typical in GMCs, the dust temperature is elevated due to the increased star formation rate (see Figure 2 of Narayanan et al. 2011a). A consequence of the increased gas temperatures and velocity dispersions in galaxy mergers is a decreased X_{CO} . This may explain the results of Downes & Solomon (1998) and Figure 1.

A second physical effect controlling the conversion factor is the gas phase metallicity. As explained before, in low-metallicity gas, the carbon resides predominantly in the form of CI or CII (rather than CO) due to photodissociation, whereas H_2 can self-shield to survive. In this regime, the velocity-integrated CO intensity decreases for a given H_2 gas mass, and the X-factor rises. MHD models of GMCs by Glover & Mac Low (2011) and Shetty et al. (2011b,a), as well as cosmological galaxy evolution simulations (R. Feldmann et al., submitted) find similar trends.

While our model isolated discs have mean X -factors comparable to the Milky Way, and our model $z=0$ major mergers have X -factors consistent with the observed range presented in Figure 1, there is no “disc” value and “merger” value of X_{CO} . In a minor merger, for example, the rise in gas temperatures and velocity dispersions are not as extreme as they are in 1:1 major merger. Hence, the rise in velocity-integrated CO intensity is not as large, and the X -factor does not decrease as much. Similarly, in high- z disc galaxies, large gas clumps that are forming stars rapidly due to gravitational instabilities in a gas-rich environment have larger temperatures and velocity dispersions than quiescent $z=0$ discs. Hence, they have X -factors lower than the locally calibrated “quiescent/disc” value. There is no “merger” value and “disc” value of X_{CO} (Narayanan et al. 2011b).

The good news is that the CO-H₂ conversion factor can be observationally calibrated. While the gas temperature and velocity dispersion are not easily observable, in our models, the CO surface brightness (line intensity) serves as a good proxy for the product of these quantities. That is, larger CO line intensities tend to correlate with larger velocity dispersions and temperatures. Fitting X_{CO} in our simulations against the CO line intensity, W_{CO} , and metallicity, we get:

$$X_{\text{CO}} = \frac{6.75 \times 10^{20} \times \langle W_{\text{CO}} \rangle^{-0.32}}{Z'^{0.65}} \quad (2)$$

$$\alpha_{\text{CO}} = \frac{10.7 \times \langle W_{\text{CO}} \rangle^{-0.32}}{Z'^{0.65}} \quad (3)$$

where $\langle W_{\text{CO}} \rangle$ is the luminosity-weighted CO intensity over all GMCs in a galaxy, and Z' is the metallicity in units of solar. In the limit of a uniform distribution of luminosity from the ISM in a galaxy, $\langle W_{\text{CO}} \rangle$ reduces to L'_{CO}/A , or the CO intensity (A is the area observed). Note the similarity of our model fit for X_{CO} , and what was derived from empirical observations in § 2. Hence, with a metallicity estimate and a CO surface brightness, one can calculate the X -factor observationally. I note that there is an implicit ceiling value of $X_{\text{CO}} = 4 \times 10^{20} \text{ cm}^{-2}/\text{K-km s}^{-1}$ ($\alpha_{\text{CO}} = 6.3 M_{\odot} \text{ pc}^{-2} (\text{K-km s}^{-1})^{-1}$) when $Z' = 1$ in Equations 2 and 3.

4. The Ramifications of This Model Form for X_{CO}

4.1. The Kennicutt-Schmidt Star Formation Relation

The usage of Equations 2 and 3 has an immediate consequence for the observed Kennicutt-Schmidt star formation relation. Recall that when a bimodal conversion factor is used for mergers and discs, a bimodal KS relation results with different normalisations for mergers and discs (centre panel of Figure 2. When utilising our continuous form for X_{CO} , this bimodality goes away.

We now turn to the right panel of Figure 2, where we have applied our model form for X_{CO} to the observed data in the Daddi et al. (2010a) and Genzel et al. (2010) compilation. The bimodal relationship is reduced to a unimodal one with best fit index is a relationship $\Sigma_{\text{SFR}} \sim \Sigma_{\text{mol}}^2$. In this picture, there are no different “modes” of star formation in mergers and discs. On *average*, mergers do form stars more efficiently than disc galaxies as they lie preferentially toward the high Σ_{SFR} regime of Figure 2. However, if one examines the central region of the fit, where both high- z discs (filled blue circles) and local galaxy mergers (open black squares) reside, it is evident that

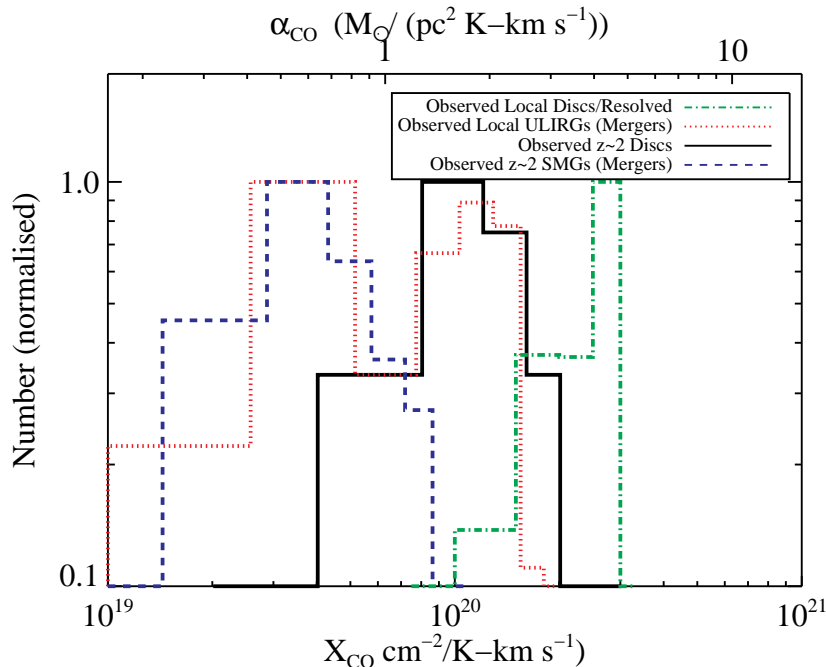


Figure 3. Histograms of the derived conversion factors for all the galaxies in Figure 2.

they have similar star formation efficiencies (defined as $\text{SFR}/M_{\text{H}_2}$). A key point of this model is that *if the physical conditions in a disc and a merger are the same, they will have the same conversion factor.*

4.2. The Typical Conversion Factors for Different Galaxy Populations

This point is made more clearly in Figure 3, where we show the conversion factors we derive for the galaxies in Figure 2 utilising Equations 2. Here, we see that *on average* mergers have lower conversion factors than discs. The high- z SMGs (blue dashed line) have the lowest X_{CO} values, followed by low- z mergers (red dotted line). However, there is substantial overlap in the conversion factors, especially between the low- z mergers and high- z discs (black solid line).

This model clearly predict, then, that attempts to determine conversion factors for high- z discs will evidence a lower average value than the Galactic mean value. A few attempts at constraining X_{CO} in high- z BzK galaxies exist. Daddi et al. (2010b) developed dynamical models for two high- z BzK galaxies. After subtracting off the measured stellar and assumed dark matter masses, they were able to derive an X_{CO} factor by relating the remaining (presumably) H_2 mass to observed CO luminosity. This method recovered a mean X-factor of $\sim 2 \times 10^{20} \text{ cm}^{-2}/\text{K-km s}^{-1}$, or $\alpha_{\text{CO}} \approx 3 M_{\odot} \text{ pc}^{-2} (\text{K-km s}^{-1})^{-1}$. Magdis et al. (2011) recovered similar results via dust to gas ratio arguments. Our model predicts that further measurements of the conversion factor from high- z discs will find a mean value a factor of a few lower than this (Figure 3).

5. Conclusions

The principal result from this work is that the CO-H₂ conversion factor in galaxies varies with the physical conditions in the galaxy. It is not bimodal with the global morphology of the galaxy. Rather, the physical environment sets the CO-H₂ conversion factor.

The dominant drivers in the conversion factor are the gas temperature, velocity dispersion and metallicity. While the former two are difficult to observe, they can be parameterised by the observable CO intensity. With this, the CO-H₂ conversion factor can be described as function of CO intensity and gas phase metallicity. We show that this function can be derived both from empirical observational results, as well as numerical modeling.

Acknowledgments. I would like to thank the organizers of the *Galaxy Mergers in an Evolving Universe* for inviting me to such an educational meeting. Thanks also to Nick Scoville for setting the tone early in the meeting that there should be no limit to the number of questions. It was fun getting to field a barrage of questions (mostly from Nick!) for 20 minutes after my talk. Thanks go to Mark Krumholz, Eve Ostriker, and Lars Hernquist who I have collaborated extensively with in developing this model. Finally, thanks to the NSF for funding this work through grant AST-1009452.

References

- Arimoto, N., Sofue, Y., & Tsujimoto, T. 1996, PASJ, 48, 275
- Bolatto, A. D., Leroy, A. K., Rosolowsky, E., Walter, F., & Blitz, L. 2008, ApJ, 686, 948. 0807.0009
- Daddi, E., et al. 2010a, ApJ, 714, L118. 1003.3889
- 2010b, ApJ, 713, 686. 0911.2776
- Downes, D., & Solomon, P. M. 1998, ApJ, 507, 615. arXiv:astro-ph/9806377
- Genzel, R., et al. 2010, MNRAS, 407, 2091. 1003.5180
- 2011, ArXiv e-prints. 1106.2098
- Glover, S. C. O., & Mac Low, M.-M. 2011, MNRAS, 412, 337. 1003.1340
- Goldsmith, P. F. 2001, ApJ, 557, 736
- Israel, F. P. 1997, A&A, 328, 471. arXiv:astro-ph/9709194
- Krumholz, M. R., Leroy, A. K., & McKee, C. F. 2011, ApJ, 731, 25. 1101.1296
- Krumholz, M. R., McKee, C. F., & Tumlinson, J. 2008, ApJ, 689, 865. 0805.2947
- 2009, ApJ, 699, 850. 0904.0009
- Krumholz, M. R., & Thompson, T. A. 2007, ApJ, 669, 289. arXiv:0704.0792
- Leroy, A. K., et al. 2011, arXiv/1102.4618. 1102.4618
- Magdis, G. E., et al. 2011, arXiv/1109.1140. 1109.1140
- Narayanan, D., Krumholz, M., Ostriker, E. C., & Hernquist, L. 2011a, MNRAS, 418, 664. 1104.4118
- Narayanan, D., Krumholz, M. R., Ostriker, E. C., & Hernquist, L. 2011b, arXiv/1110.3791. 1110.3791
- Narayanan, D., et al. 2008, ApJS, 176, 331. arXiv:0710.0384
- Ostriker, E. C., & Shetty, R. 2011, ApJ, 731, 41. 1102.1446
- Shetty, R., et al. 2011a, arXiv/1104.3695. 1104.3695
- 2011b, MNRAS, 412, 1686. 1011.2019
- Solomon, P. M., & Barrett, J. W. 1991, in Dynamics of Galaxies and Their Molecular Cloud Distributions, edited by F. Combes, & F. Casoli, vol. 146 of IAU Symposium, 235
- Springel, V. 2005, MNRAS, 364, 1105. arXiv:astro-ph/0505010
- Tacconi, L. J., et al. 2008, ApJ, 680, 246. 0801.3650
- Wolfire, M. G., Hollenbach, D., & McKee, C. F. 2010, ApJ, 716, 1191. 1004.5401